# Morphology Development of LDPE–PS Blend Compatibilization

MOHAMED TAHA[1,*] and VALÉRIE FREREJEAN[2]

[1]Laboratoire des Matériaux Macromoléculaires, bâtiment 403, URA CNRS no. 507, Institut National des Sciences Appliquées de Lyon, 20, Avenue A. Einstein, 69621 Villeurbanne Cedex, France; [2]SOREPLA, BP 89, Neufchateau Cedex, France

SYNOPSIS

LDPE–polystyrene (PS) blends were compatibilized using three PS-hydrogenated polybutadiene–PS and one PS–hydrogenated polybutadiene block copolymers. The blends were prepared by corotating twin-screw extrusion, then were injection-molded. During processing, the morphology evolution of the blends was studied using SEM and image-analyzing techniques. Different screw profiles were used for extrusion. Under the extrusion conditions and when all the blend constituents had melted, the use of one kneading-disc section resulted in a high mixing effect. The addition of other kneading-disc sections did not increase the dispersion. The flow of the blend, through the extruder die or in the injection mold, induced heterogeneous skin–core structures. The analysis of the evolution of the structure of these blends during processing showed that the addition of a compatibilizer increased their stability. Going from LDPE-rich to PS-rich blends, the morphology evolves from a nodular dispersion of PS in LDPE to a cocontinuous structure. With the addition of a copolymer to a 25–75 wt % LDPE–PS blend, the structure changes from a cocontinuous to a nodular one. Comparing the effect of the different copolymers on the blend morphology, the diblock copolymer results in the most homogeneous and finest dispersions. The stabilization of increasing potential values of the interface surface of these blends requires increasing concentrations of the copolymers. © 1996 John Wiley & Sons, Inc.

## INTRODUCTION

Blending immiscible polymers for the development of new materials with good performance is often used as an alternative to the synthesis of new polymers, for the preparation of new materials, or for the modification of specific properties of some polymers. For this reason, a large number of studies have been devoted to polymer blends.[1–5] It is well established that the performance of blend-issued materials depends on the physical properties of the different constitutive polymers, the processing history, and the multiphase interface.[6–13] The principal parameters governing the effectiveness of mixing and controlling the morphology of a dispersed phase are the viscosity ratio, the interfacial tension, and the processing history.[14–16]

Due to the deformable nature of the minor phase of an immiscible blend, a wide range of sizes and shapes can be generated during processing. Generally, a blend of immiscible polymers leads to a material with poor dispersion, low interfacial adhesion, and, consequently, poor mechanical properties. Compatibilization agents are often used to improve the dispersion and interfacial cohesion of these blends, consequently increasing the mechanical properties of the issued material.[1,2]

With the growing interest in plastic waste recovery, two recycling strategies exist: One implies a separation step, generally leading to a blend containing a major polymer with small proportions of other polymers, metals, and papers. The other is to use a plastic mixture without any separation. Whatever the strategy used, a raw material issued

* To whom correspondence should be addressed.

Journal of Applied Polymer Science, Vol. 61, 969–979 (1996)
 CCC 0021-8995/96/060969-11

**Table I Materials Used for Blend Preparation**

| Name | Code | $\overline{M_n}$ (g mol$^{-1}$) | $I$ | MFI (g/10 min) | Origin |
|---|---|---|---|---|---|
| Low-density polyethylene | LDPE | 22500 | 9.9 | 7 | ENICHEM (MP20) |
| Polystyrene | $PS_1$ | 127000 | 2.2 | 1.7 | ELF ATOCHEM (Lacqrene 1170) |
| | $PS_2$ | 85600 | 2.5 | 11 | ELF ATOCHEM (Lacqrene 1540) |
| Polystyrene-hydrogenated polybutadiene-polystyrene block copolymer | KG50 | 17400 | | | SHELL (Kraton G 1650) |
| | KG51 | 7400 | | | SHELL (Kraton G 1651) |
| | KG52 | 52000 | | | SHELL (Kraton G 1652) |
| Polystyrene-hydrogenated polybutadiene block copolymer | KG01 | 22000 | | | SHELL (Kraton G 1701) |

from plastic waste generally consists of a polymer blend.

Polyethylene (PE) and polystyrene (PS) are often present as a mixture in recycled polymers. These blends are widely described in the literature[7,10,17-24] and are often prepared using a solvent, internal mixers, and compression molding,[17,18] a single-screw extruder,[19] and a twin-screw extruder.[10,24] Only a little information is given concerning the morphology evolution of these blends during the different steps of processing, and the morphology of the obtained materials is rarely quantified.

In this study, we considered the morphological evolutions of LDPE–PS blends during twin-screw extrusion and injection molding. We inspected the mixing efficiency of the kneading disks of a corotating twin-screw extruder and the limits of processing conditions on dispersion. Then, we quantified the compatibilization effect of different block copolymers on the morphology of the blends and their stability during processing.

## EXPERIMENTAL

Materials used in this study are presented in Table I. Polymer compounding was done using a CLEXTRAL BC21 intermeshing corotating twin-screw extruder ($D$ = 25 mm, $L$ = 900 mm). Polymer pellets were first dry-blended with a compatibilizer, then fed into the extruder hopper. The extruder drive was run at the desired speed (300 rpm when not specified in the text). It took approximately 10 min for the temperature and pressure to be stabilized. Then, the extrudate was passed through a water bath, dried in a hot air stream, and pelletized.

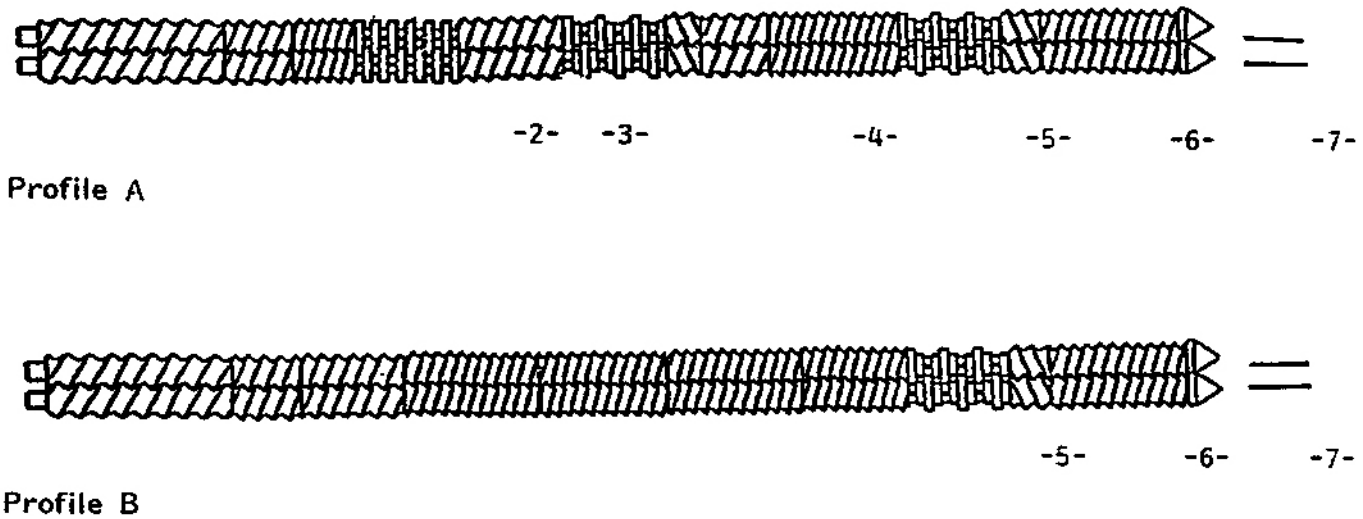


**Figure 1** Screw profiles used for blend preparation.

**Table II Residence Time Distribution of $PS_1$ Extrusion at 190°C**

| Exp. No. | Screw Profile | $N$ (rpm) | $Q$ (kg/h) | $t_m$ (s) | $\sigma_t^2$ ($\sigma 2$) | $T_m$ (s) |
|---|---|---|---|---|---|---|
| 1 | A | 300 | 8 | 56 | 438 | 50 |
| 2 | B | 300 | 8 | 62 | 217 | 61 |
| 3 | B | 50 | 1.3 | 286 | 3869 | 297 |

In the case where samples were to be removed for morphological studies, the extruder screw rotating was stopped and the cooling system of all barrels switched on. At the same time, the barrels, positioned on a bar driven by a hydraulic jack, were quickly removed and specimens directly quenched with cold water.

For residence time distribution studies, biphenyl was used as a UV tracer. As an impulse, 0.5 g were injected into the feed hopper to the extruder. Samples were collected from the extruder die, diluted in THF, and analyzed by SEC with a UV detector at 254 nm. The tracer concentrations in the sample collected at time $t(C_t)$ were measured using a calibration curve. The extruder response to the inlet pulse $E_t$ and the cumulative distribution $F_t$ are expressed in eqs. (1) and (2) ($\Delta t$ is the time interval between successive sampling):

$$E_t = \frac{C_t}{\sum_0^\infty C_t \cdot \Delta t} \quad (1)$$

$$F_t = \sum_0^t E_t \cdot \Delta t \quad (2)$$

Specimens, for mechanical measurement (dog bones, ISO 60), were prepared by injection molding of extruded pellets using a BILLION 140T press. The maximum barrel temperature was set at 190°C and the mold cooled by cold water.

The image analysis system was composed of a 512 × 512 square pixels CCD camera (PULMIX TM760), a frame grabber (Digital Vision Cyclope 600), and home-made software. Scanning electron microscopy was carried out on liquid nitrogen-fractured surfaces using a JEOL JM-810A microscope.

## RESULTS AND DISCUSSION

### Morphology Evolution During Processing

The mechanical properties of materials prepared from immiscible polymer blends are directly related to the microscopic morphology and the interphase cohesion. This morphology results not only from the mixing operation, but also from the flow of the blends in the die, when they are extruded, or from the mold-filling conditions when they are injection-molded.

The importance of corotating twin-screw extrusion in polymer compounding has induced intensive activity in extrusion modeling. On the basis of these fundamental studies and experimental investigations, the importance of kneading disks on blend dispersion is clearly established.[25–27] The final morphology results from a dispersed phase division–coalescence equilibrium during the blending operation.[15,16] The optimization of a screw profile, devoted to polymer mixing, is established when this equilibrium is obtained at the die entrance.

In this study, we chose two screw profiles for blend compounding. Screw profile A has three kneading block areas: the second and the third, going from the feed hopper, are followed by a left-handed screw element. Screw profile B contains only one kneading block followed by a left-handed screw element (Fig. 1).

### *Residence Time Distribution*

Before considering the LDPE–PS compounding, it is important to compare the residence time distribution of products (RTD) when profiles A and B are used for extrusion. We must note that this RTD will depend on the rheology of the studied systems and, consequently, each blend will have a different RTD. For this study, we chose to measure the $PS_1$ extrusion RTD. The obtained results have only an indicative value. We calculated, using the tracer method, the mean residence time:

$$t_m = \sum_0^\infty t \cdot E_{(t)} \cdot \Delta t \quad (3)$$

and the second moment or variance:

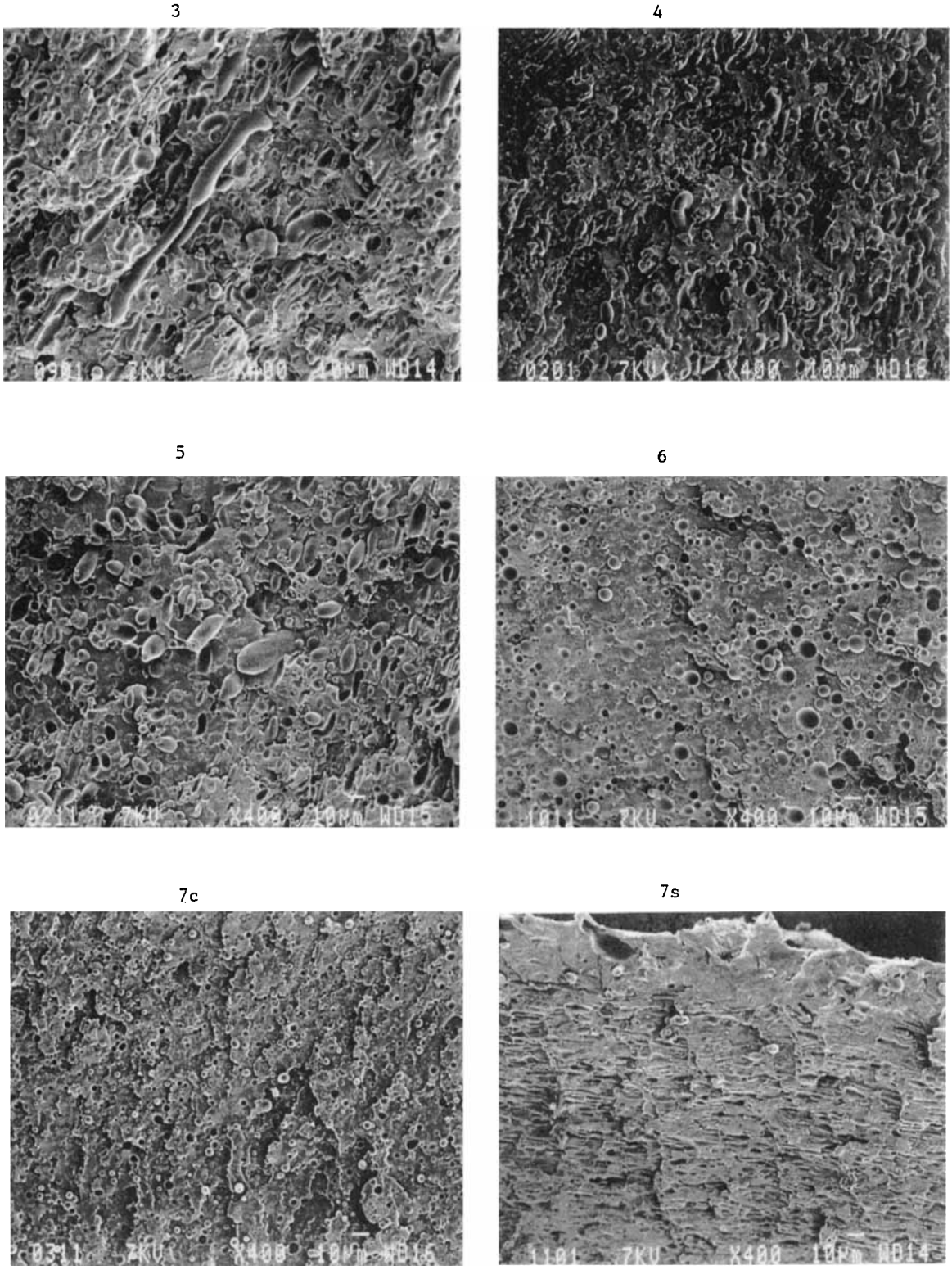


**Figure 2** Morphology evolution during 75–25 wt % LPDE–$PS_1$ blend extrusion on points 3–7. Points 7c and 7s correspond, respectively, to the core and surface of the extrudate at the die exit. Profile A, 300 rpm, 8 kg $h^{-1}$, 190°C.

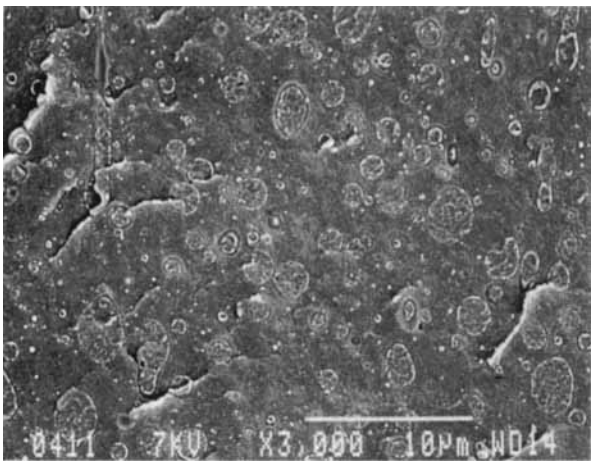


**Figure 3** 75–25 wt % LDPE–PS blend compatibilized by 5 pcr of KG50. Profile A, 300 rpm, 8 kg $h^{-1}$, 190°C.

$$\sigma_t^2 = \sum_0^\infty (t - t_m)^2 \cdot E_{(t)} \cdot \Delta t \qquad (4)$$

Another way to calculate the mean residence time ($T_m$) is to use

$$T_m = \frac{m}{Q} \qquad (5)$$

where $m$ is the mass of the product within the extruder screws and $Q$ is the throughput.

The results are given in Table II. We note that the two methods used for the measuring of the mean residence time lead to approximately the same value. However, the use of the tracer method gives additional information concerning the distribution.

We see that, even if the mean residence time is approximately the same at 300 rpm for profiles A and B, the RTD are very different. Examining the values of the variance (Table II), we see clearly that the addition of kneading discs in profile A leads to a broader distribution compared to the one obtained with profile B. This means that the blends prepared using profile A are more heterogeneous, in terms of mixing history, than those prepared with profile B.

Comparing experiments 2 and 3 (Table II), we verify that the extrusion experiments, made at a constant $Q/v$ (where $v$ is the screw speed), lead to the same screw filling (110 g). However, as expected, the mean residence times are very different: When $v$ is divided by 6, $t_m$ is multiplied by approximately 6.

### *Morphology Evolution During the LDPE–PS Blend Extrusion with Profiles A and B*

The design of a screw configuration of a corotating twin-screw extruder, devoted to a mixing operation of immiscible polymers, is made to provide enough energy for the required shear and mixing effect. Successive kneading sections, as designed in profile A, are often used to increase the energy input to the process, supposing that this will lead to a high level of dispersion.

The beneficial dispersion effect of kneading discs is accompanied by an increase in temperature through viscous dissipation. Combined with the high shearing levels that they introduce, they can cause the degradation of heat- and shear-sensitive polymers. Even when the processed polymers are relatively stable polymers, excessive shearing can damage them. For this reason, the dispersive effect of kneading discs, and, consequently, the energy introduced by their use, must be optimized. Important information concerning the location and quantity of kneading areas, necessary for the blending process, can be obtained by a direct analysis of the morphology evolution of the blends using profiles A and B.

Profile A was first used to study the morphology development during the extrusion of 75–25 wt % LDPE–$PS_1$ blends. Sampling points are shown in Figure 1. SEM images of the specimens are given in Figure 2. LDPE melts at the end of the first kneading disc area, at point 2. PS was completely plasticized in the second kneading section (point 3). The morphology analysis of the blend before the complete plasticizing of PS (point 2) showed the coexistence of lamellar and spherical dispersions of PS in the LDPE matrix. This morphology results from laminar mixing in the melt conveying zone. At this point, the morphology is analogous to the one expected in a melting zone of a single-screw extruder. This result is not surprising and confirms the transport and dispersion analogy between the forward conveying screw elements of a corotating twin-screw extruder and a single-screw extruder.[14,27] In points 4 and 6, we have almost the same morphology: a spherical dispersion of PS in LDPE. At points 3 and 5, we also have an equivalent morphology: a spherical dispersion of PS in LDPE and some ellipsoidally shaped PS dispersions. This shows that the third kneading disc area is useless.

After the blend was passed through the die, an inhomogeneous core–skin morphology was obtained: At the center of the extrudate, a spherical dispersion,

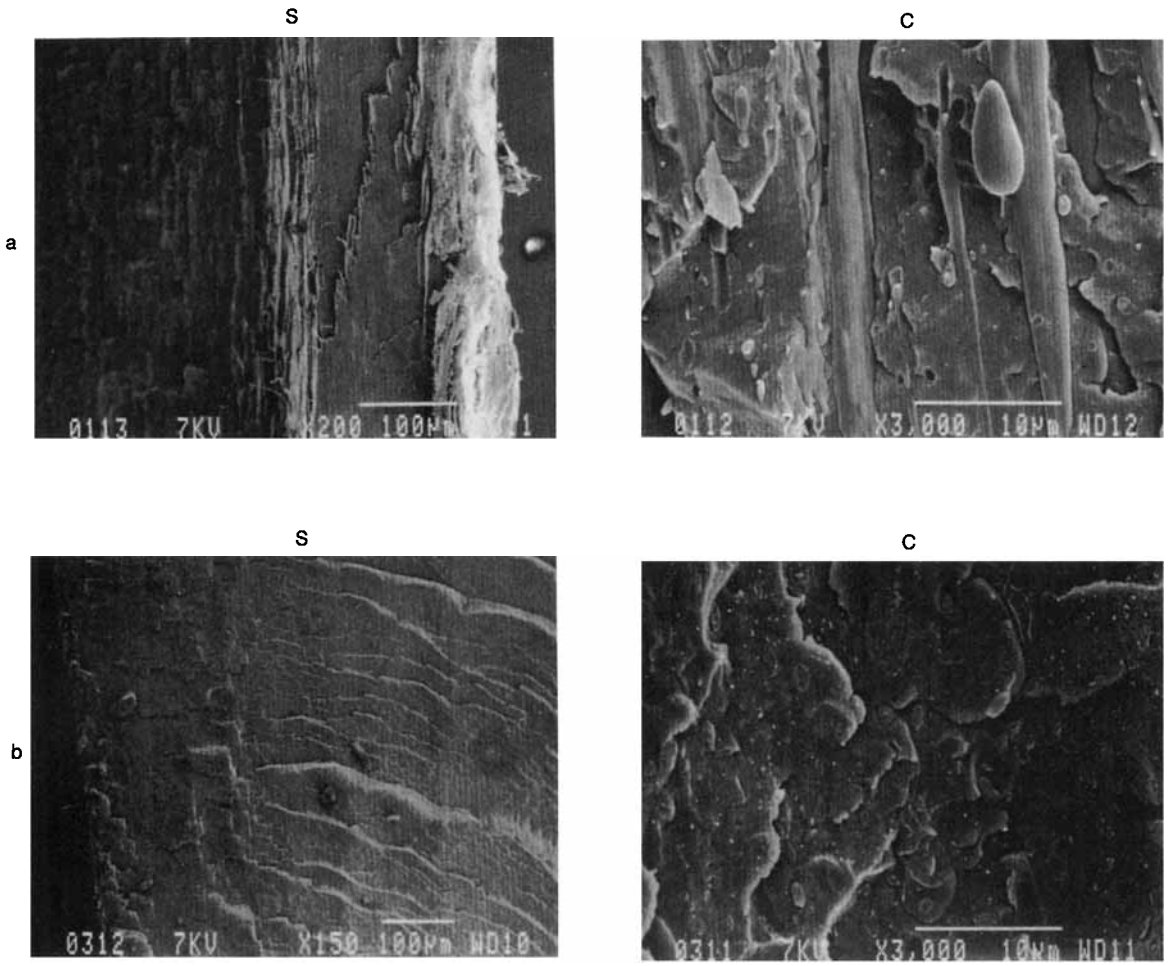


**Figure 4** Injection-molded 75–25 wt % LDPE–PS blends: (a) noncompatibilized; (b) compatibilized by 5 pcr KG50. s, surface of the specimen; c, core of the specimen.

with a smaller diameter than at point 6, and near the surface, an ellipsoidally shaped dispersion. This inhomogeneity is a consequence of the different shear rates in the core and skin parts and, given the high quenching effect of the used cold water, can reasonably describe the polymer blend flux morphology.

With the addition of 5% KG50, the morphology development in the extruder changed considerably, and no morphological difference was observed at points 3–6 or at the core of extrudate issued at the die exit (Fig. 3). In this case, we note that the morphology equilibrium is obtained faster than when no compatibilizer was added and that the morphology is more stable. Comparing the SEM morphologies of compatibilized and noncompatibilized blends (Figs. 2 and 3), we can see clearly that in the compatibilized blends the nodules are cut in two, while they are pulled out in the noncompatibilized blend. This indicates a poor interphase adhesion in the noncompatibilized blend and a relatively high interfacial cohesion for the compatibilized one. Using screw profile B, for noncompatibilized and compatibilized blends, we obtain the same morphologies at point 6 as with profile A.

These experiments showed that in the extrusion conditions used (i) the morphology equilibrium was obtained, as soon as the blend constituents were plasticized, with the use of one kneading disc area and (ii) the mixing performance of profiles A and B are equivalent. For these reasons, and to preserve the blend components from unnecessary shearing, we continued our study with profile B.

### *Injection-molded Blend Morphology*

During injection, a part of the material freezes on the mold surface and the frozen layer thickness

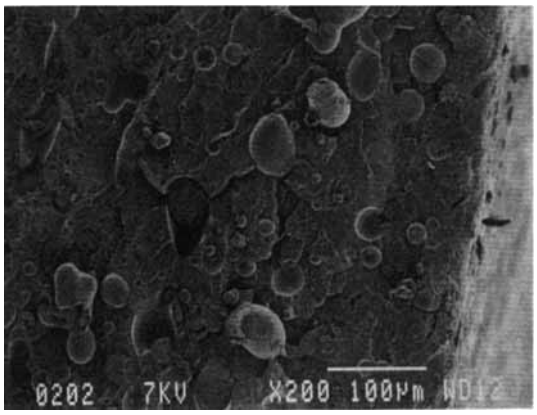


a

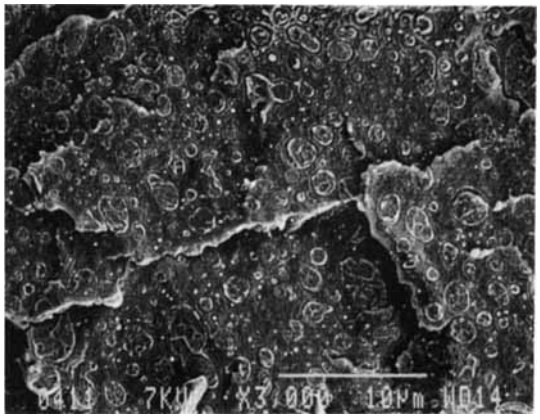


b

**Figure 5** The same blends as in Figure 4, annealed for 10 min at 190°C.

changes during injection.[28] The molded polymer morphology results from a succession of parts frozen during injection, under different shear rates at different temperatures, and a core part frozen after the complete injection.

The resulting complex morphologies are particularly conspicuous when some blends are injection-molded. To illustrate this and to study the morphological evolution difference between the noncompatibilized and compatibilized blends, two blends were prepared by twin-screw extrusion, dried, and injection-molded to give dog bones. The first one is a 75/25 wt % LDPE/$PS_1$; the second blend corresponds to the first one compatibilized by 5 pcr of KG50.

In the first injection-molded blend, three different zones can be discerned. In three of them, a clear orientation of PS in the flow direction is observed (Fig. 4).

In the skin area, we have a lamellar structure. In the intermediate one, fibers are observed. In the core part, ellipsoidal, and threadlike droplets are observed. The injection-molded blend 2 showed a lower orientation. In the skin part, a lamellar structure is observed. The intermediate part contains only ellipsoid particles, and in the core part, we only have spherical and ellipsoidal droplets. In the skin part, the structure of the blend was quenched by rapid cooling, and the structure observed is representative of the flux morphology in this area.

Under the injection conditions, the core part of specimens is liquid for a relatively long time and the morphology is not readily quenched and the structure observed is different from the flux morphology. A spontaneous change of morphology occurs after injection in order to minimize the interfacial area. For compatibilized blends, this morphological evolution can be achieved during the time the core is still liquid. For the noncompatibilized blends, the center is not liquid long enough to complete the reorientation of the dispersion.

The two specimens were prepared under the same conditions, and we can reasonably suppose that the core of both of them is liquid for the same time. This indicates that reorientation needs less time for the compatibilized blend than for the noncompatibilized one.

To complete these observations, specimens of each blend were annealed for 20 min at 190°C and cooled slowly. The morphology on the fracture surface showed only spherical droplets (Fig. 5). For the noncompatibilized blend, the droplets were approximately 10 times larger than those present at the extruder die. This shows that important coalescence events occurred during injection or annealing. For the compatibilized blend, the droplet dimensions were of the same order of magnitude as those observed from the extruder die. In this case, if we have coalescence during injection, division occurs during annealing, leading to a morphology equivalent to the one we had before injection. These observations confirm the higher morphological stability of the compatibilized blend and its lower interface tension.[1,2]

## LDPE–PS Morphology Evolutions with Blend Compositions

Information concerning the effect of different copolymers on the morphology of these blends can be

**Table III Image Analysis Results Concerning 72/25 Wt % LDPE/PS Blends**

| Blend | Copolymer | Copolymer (Wt %) | Copolymer (mol %) | $\overline{D_n}$ ($\mu$m) | $\overline{D_w}$ ($\mu$m) | $I$ | % Variation $\overline{D_n}$ | $Sv$ ($\mu m^2/\mu m^3$) |
|---|---|---|---|---|---|---|---|---|
| 75–25 wt % LDPE–$PS_1$ | | 0 | 0 | 2.1 | 3.4 | 1.6 | — | 0.35 |
| | | 1 | 0.13 | 0.89 | 1.24 | 1.39 | −0.98 | 0.98 |
| | | 3 | 0.39 | 0.45 | 0.55 | 1.23 | −2.29 | 2.29 |
| | KG1701 | 5 | 0.64 | 0.59 | 0.64 | 1.1 | −1.5 | 1.5 |
| | | 7 | 0.90 | 0.19 | 0.22 | 1.18 | −4.5 | 4.5 |
| 75–25 wt % LDPE–$PS_1$ | | 1 | 0.54 | 0.69 | 1.16 | 1.67 | −0.77 | 0.77 |
| | | 3 | 1.60 | 0.65 | 1.43 | 2.19 | −0.67 | 0.67 |
| | KG52 | 5 | 2.64 | 0.638 | 1.65 | 2.41 | −0.62 | 0.62 |
| | | 7 | 3.65 | 0.52 | 0.88 | 1.67 | −0.75 | 1.12 |
| 75–25 wt % LDPE–$PS_1$ | KG 51 | 5 | 0.81 | 1.40 | 2.11 | 1.51 | −33 | 0.45 |
| | | 7 | 1.13 | 0.69 | 1.17 | 1.71 | −67 | 0.77 |
| 75–25 wt % LDPE–$PS_1$ | | 1 | 0.38 | 0.91 | 1.73 | 1.9 | −75 | 0.67 |
| | | 3 | 1.14 | 0.68 | 1.22 | 1.79 | −68 | 0.82 |
| | KG50 | 5 | 1.88 | 4.48 | 0.84 | 1.72 | −77 | 1.16 |
| | | 7 | 2.62 | 0.30 | 0.40 | 1.31 | −86 | 3.0 |
| 75–25 wt % LDPE–$PS_2$ | | 0 | 0 | 1.5 | 2.7 | 1.78 | — | 0.48 |
| | KG52 | 3 | 1.55 | 0.51 | 0.97 | 1.93 | −66 | 1.15 |
| | | 5 | 2.56 | 0.49 | 0.78 | 1.61 | −67 | 1.18 |

obtained using the quantitative image analysis of SEM cryofractured surfaces. Since spherical PS dispersions are obtained for blends containing 75–25 wt %, respectively, LDPE/$PS_1$ and LDPE/$PS_2$, simple diameter measurements can be used. We can calculate a number-average diameter ($\overline{D_n}$),

$$\overline{D_n} = \frac{\sum n_i D_i}{\sum n_i} \tag{6}$$

and a weight-average diameter ($\overline{D_w}$),

$$\overline{D_w} = \frac{\sum n_i D_i^2}{\sum n_i D_i} \tag{7}$$

These dispersions can also be analyzed using the interfacial surface area ($Sv$) (Table III). The mechanism of deriving $\overline{D_n}$, $\overline{D_w}$, and $Sv$ was well explained by Dehoff and Rhines.[29]

First, we note that the dispersion of $PS_1$ and $PS_2$ in LDPE is very different (Table III). Smaller nodules are obtained when $PS_2$ is used. This can easily be explained comparing the viscosity ratio of PS to LDPE ($\eta$PS/$\eta$LDPE). This viscosity ratio, closer to 1 when $PS_2$ is used, results in a smaller Weber number and, consequently, in finer dispersion.[30]

To compare the copolymer effect on LDPE/$PS_1$ blends, we can plot $\overline{D_n}$ evolution with the weight concentration of these copolymers [Fig. 6(a)]. The effect of the copolymers used can be classified into two categories: For KG50, KG52, and KG01, an important decrease of $\overline{D_n}$ is observed for relatively low concentrations; diameters then remain stable. The KG51 effect is very different from the others. For low concentrations, up to 3%, the blend structure is very complex and a nodular structure is obtained only for a higher concentration (5%). The obtained $\overline{D_n}$ with KG51 are somewhat higher than those we have with other copolymers.

Since the molar masses of the copolymers used are very different, and if we want to compare their efficiency as compatibilizing agents, the PS dispersion evolution with the molar concentrations of the different copolymers is more significant [Fig. 6(b)].

We can clearly see here that the diblock copolymer KG01 is the most efficient copolymer for PS dispersion. This effect can be attributed either to the diblock structure of KG01 compared to the triblock structure of the other copolymers or to the similar molar mass of the diblocks of KG01 toward those of the blend constituents. Comparing the three triblock copolymers, the KG52 and KG50 dispersion

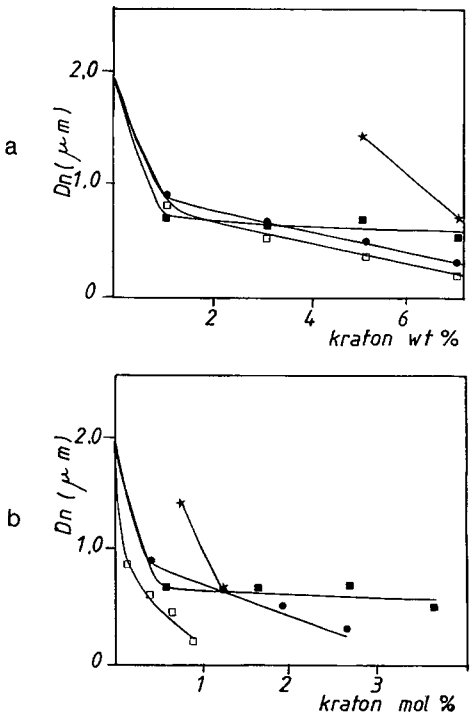


**Figure 6** $\overline{D_n}$ of the PS dispersion in 75–25 wt % LDPE–PS compatibilized blend. Profile A, 300 rpm, 8 kg $h^{-1}$ output, 190°C: (a) wt %; (b) mol %; (●) KG50; (★) KG51; (■) KG52; (□) KG01.

effect is important and similar for low concentrations (0.5 mol %). For K52, no evolution is obtained for higher concentrations, while a small regular decrease is obtained for KG50. We can also note that a similar effect is obtained with the addition of 1 mol % whatever is the triblock copolymer used.

Other aspects concerning these dispersions are studied using the cumulate distribution function (Fig. 7). When KG52 is used, a large dispersion evolution is obtained with the addition of 1 wt %. For higher copolymer concentrations, only slow dispersion evolutions are observed. The effect of KG51 is quite different. Even when we add 5 wt % of KG51, the cumulate distribution of the smaller nodules is equivalent to the one that we have when no copolymer is used, and the only evolution observed concerns the size decrease of the bigger nodules. A more significant evolution is observed when 7 wt % KG51 is added. In this case, the dispersion becomes much finer than when no copolymer is used. Regular evolutions are observed with the addition of increasing amounts of KG01 and KG50. We also note that the dispersions are finer when KG01 is used.

If we examine these cumulate distribution evolutions with the molar % of the added copolymer, the singular effect of KG01 is evident. In this case, all the nodules of PS have a diameter smaller than 0.5 μm when 0.9 mol % is added. When other copolymers are used with an equivalent molar concentration, the maximum dispersion diameter is 3 μm. The dispersity ratio ($Ip$) also gives information concerning the dispersion width:

$$Ip = \frac{\overline{D_w}}{\overline{D_n}} \tag{8}$$

The results are in Table II. Only with KG01 do all the distributions of compatibilized blends have a lower $Ip$ than that of the noncompatibilized blend.

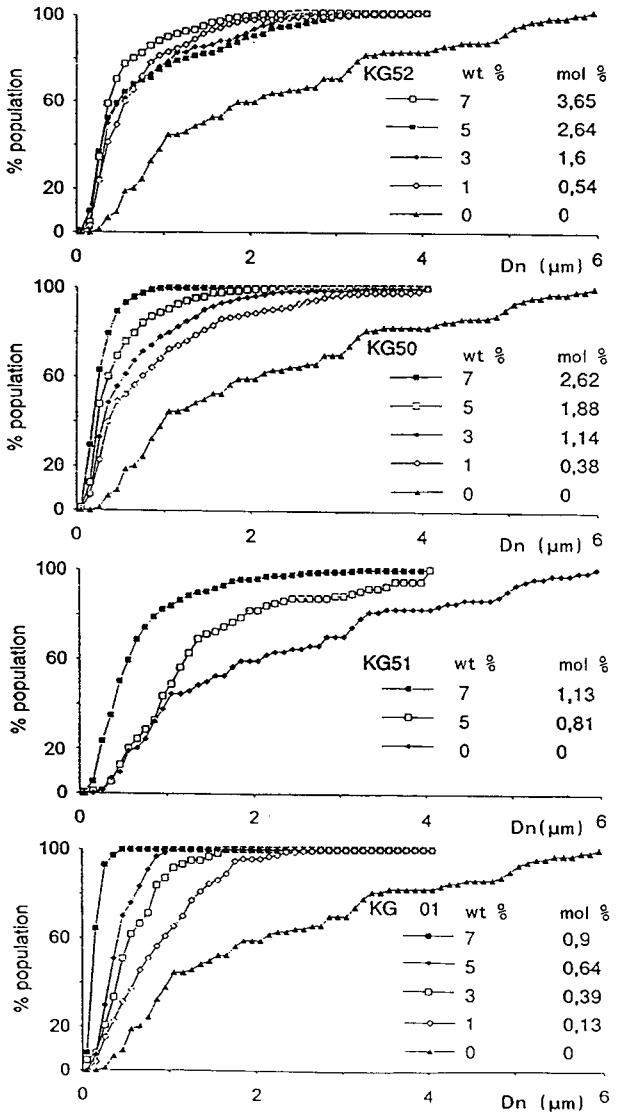


**Figure 7** $\overline{D_n}$ cumulate distributions of 75–25 wt % LDPE–PS.

All these observations show clearly that KG01 has the highest dispersion effect of the copolymers used and leads to the most homogeneous blend.

### Morphology Evolution of LDPE–PS Blends with the Homopolymer Composition

LDPE/$PS_1$ shows a nodular dispersion of PS in LDPE in LDPE-rich blends (Fig. 2). For richer PS compositions, more complex morphology is obtained, leading progressively to a cocontinuous structure (Fig. 8). It is important to note that, even for the 25–75 wt % LDPE–PS blend, we did not observe any phase inversion leading to an LDPE dispersion in a PS matrix. This can be explained by a higher spreading coefficient of LDPE around PS than the spreading coefficient for PS around LDPE.[31] For the 25–75 wt % LDPE/PS blend, a nodular dispersion is observed only when high concentrations of KG50 are added.

A good way to compare all these different morphologies is to use $Sv$. In Figure 9, the $Sv$ evolution of these blends with the addition of KG50 is reported. The 75–25 and 25–75 wt % LDPE–PS blends have an equivalent potential $Sv$. Comparing the $Sv$ evolution of these blends, we have a higher effect of KG50 on the LDPE-rich blend. This is also a consequence of the higher spreading coefficient of LDPE around PS than the contrary. For the 50–50 LDPE–PS blend, a slow evolution of $Sv$ is obtained up to a 5% copolymer addition. When 7% of copolymer is added, a large increase of $Sv$ is observed. For this blend, the potential interface area is higher than for the other blends and needs higher copolymer concentration in order to be stabilized.

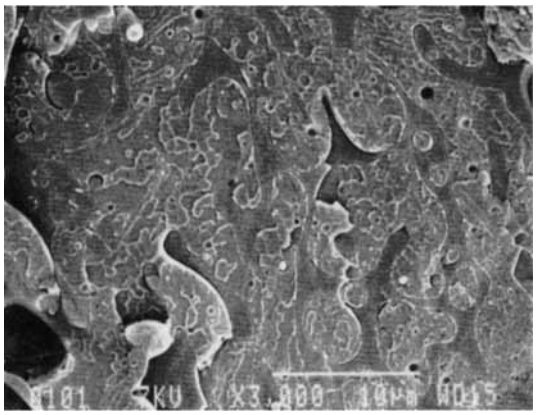

**Figure 8** Morphology of 25–75 wt % LDPE–$PS_1$ blend.

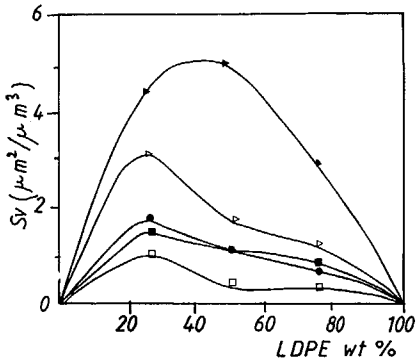


**Figure 9** Interface surface ($Sv$) evolution of LDPE/$PS_1$ (□) noncompatibilized and blends compatibilized using (■) 1, (●) 3, (▷) 5, and (▶) 7 pcr of KG 50.

## CONCLUSION

Corotating twin-screw extrusion is an efficient process for LDPE–PS blending. When all the blend constituents are plasticized, the use of one short kneading disc block leads to an equilibrium due to coalescence–division events. Comparing the effect of addition of SEBS triblock and SEB diblock copolymers shows that the finest and more stable dispersions are obtained with the diblock copolymer. The quantity of copolymers needed for the stabilization of these blends increase with the potential interface surface area. Future studies concerning these blends deal with the morphological, rheological, and mechanical property relationships of these blends.

## REFERENCES

1. D. R. Paul and S. Newman, *Polymer Blends,* Academic Press, San Diego, New York, 1978.
2. L. A. Utracki, *Polymer Alloys and Blends, Thermodynamics and Rheology,* Hanser, Munich, Vienna, New York, 1989.
3. M. Kryszewski, A. Galeski, and E. Martuscelli, *Polymer Blends,* Plenum, New York, 1984.
4. C. Keith Riew, *Rubber-Toughening Plastic,* American Chemical Society, Washington, DC, 1989.
5. H. Mark, N. Bikales, C. C. Overberger, and C. Menges, *Encyclopaedia of Polymer Science and Engineering,* Wiley-Interscience, New York, 1988.
6. R. Fayt, R. Jérôme, and P. Teyssié, *J. Polym. Sci. Polym. Lett. Ed.,* **19,** 79 (1981).
7. R. Fayt, R. Jérôme, and P. Teyssié, *J. Polym. Sci. Part B Polym. Phys.,* **27,** 775 (1989).
8. C. R. Lindsey, D. R. Paul, and J. W. Barlow, *J. Appl. Polym. Sci.,* **26,** 1 (1981).

9. B. Boutevin, Y. Pietrasanta, and T. Sarraf, *Angew. Makromol. Chem.*, **162,** 175 (1988).
10. C. C. Chen and J. L. White, in *ANTEC,* Montreal, 1991.
11. V. Bordereau and L. A. Utracki, *Polym. Eng. Sci.,* **32**(24), 1846 (1992).
12. B. D. Favis, *J. Appl. Polym. Sci.,* **39,** 285 (1990).
13. S. Thomas and R. E. Prud'homme, *Polymer,* **32**(20), 4260 (1992).
14. C. Rauwendaal, *Mixing in Polymer Processing,* Marcel Dekker, New York, 1991.
15. L. A. Utracki and Z. H. Shi, *Polym. Eng. Sci.,* **32**(24), 1824 (1992).
16. L. A. Utracki and Z. H. Shi, *Polym. Eng. Sci.,* **32**(24), 1834 (1992).
17. M. Saleem and W. E. Baker, *J. Appl. Polym. Sci.,* **39,** 655 (1990).
18. A. Ram, M. Narkis, and J. Kost, *Polym. Eng. Sci.,* **17,** 274 (1977).
19. C. R. Lindsey, D. R. Paul, and J. W. Barlow, *J. Appl. Polym. Sci.,* **26,** 1 (1981).
20. J. W. Teh and A. Rudin, *Polym. Eng. Sci.,* **31,** 1033 (1991).
21. S. Blacher, F. Brouers, R. Fayt, and P. Teyssié, *J. Polym. Sci. Part B Polym. Phys.,* **31,** 655 (1993).
22. W. E. Baker and M. Saleem, *Polym. Eng. Sci.,* **27,** 1634 (1987).
23. M. Saleem and W. E. Baker, *J. Appl. Polym. Sci.,* **39,** 655 (1990).
24. L. Yang, T. G. Smith, and D. Bigio, in *Polym. Proc. Soc. Meet.,* Akron, 1994.
25. J. L. White, *Twin-Screw Extrusion: Technology and Principles,* Hanser, New York, 1991.
26. D. Bigio and L. Erwin, *ANTEC Technical Papers,* 1987.
27. D. B. Todd and D. K. Bauman, *ANTEC Technical Papers,* 1976.
28. J. R. A. Pearson, *Mechanics of Polymer Processing,* Elsevier, London, New York, 1986.
29. R. T. Dehoff and F. N. Rhines, Microscopie quantitative, Masson, Paris, 1972.
30. H. Karam and J. C. Bellinger, *Ind. Ing. Chem. Fundam.,* **7,** 576 (1968).
31. L. A. Utracki and P. Sammit, *Polym. Eng. Sci.,* **28**(21), 1405 (1988).

*Received January 12, 1995*
*Accepted December 7, 1995*